



# Innovative Agrowaste Banana Peel Extract-Based Magnetic Iron Oxide Nanoparticles for Eco-Friendly Oxidative Shield and Freshness Fortification

Johar Amin Ahmed Abdullah<sup>1</sup> · Silvia Nicole Pérez Lagos<sup>2</sup> · Emanuel Josué Estrada Sanchez<sup>2</sup> · Octavio Rivera-Flores<sup>2</sup> · Marlon Sánchez-Barahona<sup>2</sup> · Antonio Guerrero<sup>1</sup> · Alberto Romero<sup>3</sup>

Received: 16 January 2024 / Accepted: 23 April 2024  
© The Author(s) 2024

## Abstract

This study presents the synthesis of agro-waste banana peel extract-based magnetic iron oxide nanoparticles (BPEX-MIONPs), emphasizing antioxidant capacity and food preservation. Using iron (III) chloride hexahydrate ( $\text{FeCl}_3 \cdot 6 \text{H}_2\text{O}$ ) as a precursor and a reducing agent from agro-waste peel extract, a precisely controlled process yielded BPEX-MIONPs. Characterization involved X-ray diffraction (XRD), transmission electron microscopy (TEM), scanning electron microscopy (SEM), and Fourier-transform infrared spectroscopy (FTIR). XRD revealed tetragonal  $\text{Fe}_2\text{O}_3$ , cubic magnetite structure, and monoclinic  $\text{Fe}_x\text{O}_y$ -NPs with an average size of 14.8 nm. TEM and SEM revealed diverse morphologies. TEM displayed both spherical and elongated nanoparticles, with some appearing as thin fibrils. In contrast, SEM images depicted an array primarily consisting of spherical nanoparticles, resembling coral reef formations. FTIR confirmed Fe–O bonds ( $1000\text{--}400 \text{ cm}^{-1}$ ). The antioxidant assessment showed robust DPPH free radical scavenging; BPEX achieved 100% inhibition at 18 min, and BPEX-MIONPs had an  $\text{IC}_{50}$  of  $\sim 136 \mu\text{g/mL}$ . BPEX-MIONPs, stabilized with banana-based bioplastic, effectively preserved grapes, reducing weight loss to 6.2% on day 3, compared to the control (19.0%). This pioneering study combines banana peel antioxidants with magnetic iron oxide nanoparticles, providing sustainable solutions for food preservation and nano-packaging. Ongoing research aims to refine conditions and explore broader applications of BPEX-MIONPs.

**Keywords** Antioxidant · Banana peel extract · Food preservation · Magnetic iron oxide · Nanocomposites · Sustainable materials

## Introduction

Nanoscience, focusing on materials with dimensions ranging from 1 to 100 nm, has witnessed significant growth in recent years (Beyene et al., 2017). Metal nanoparticles, in particular, have gained significant attention due to their wide

range of applications in various industrial sectors (Jurkow et al., 2020; Pardo et al., 2022). These nanoparticles, with their unique physical and chemical properties, hold promise in fields such as medicine, electronics, catalysis, and environmental remediation (Bissessur, 2020; Fahmy et al., 2016). Despite the vast array of metal nanoparticles, iron

✉ Johar Amin Ahmed Abdullah  
jabdullah@us.es

Silvia Nicole Pérez Lagos  
silvia.perez@unah.hn

Emanuel Josué Estrada Sanchez  
emanuel.estrada@unah.uh

Octavio Rivera-Flores  
jorivera@unah.edu.hn

Marlon Sánchez-Barahona  
marlon.sanchez@unah.edu.hn

Antonio Guerrero  
aguerrero@us.es

Alberto Romero  
alromero@us.es

<sup>1</sup> Departamento de Ingeniería Química, Escuela Politécnica Superior, Universidad de Sevilla, 41011 Sevilla, Spain

<sup>2</sup> Unidad de Gestión de Investigación Científica, Ingeniería Agroindustrial, Universidad Nacional Autónoma de Honduras Tecnológico Danlí, Danlí 13201, Honduras

<sup>3</sup> Departamento de Ingeniería Química, Facultad de Química, Universidad de Sevilla, 41012 Sevilla, Spain

oxide nanoparticles (IONPs) stand out due to their exceptional thermal, optical, electronic, and superparamagnetic properties (Patra & Baek, 2017; Ramananda et al., 2023). This has led to intensified research efforts aimed at synthesizing and characterizing IONPs for various applications. Moreover, the natural occurrence of IONPs, along with their synthesis through diverse methods, results in a wide range of crystal structures and iron valence states. These variations in structure and composition contribute to the diverse magnetic properties exhibited by IONPs, including saturation magnetization, coercivity, and remanence (Abdullah et al., 2020).

Magnetic iron oxide nanoparticles (MIONPs), one of the most commonly used nanoparticles, have found widespread applications due to their unique characteristics, including specificity, magnetism, and biocompatibility (Bhole et al., 2023). While physical and chemical methods have traditionally been employed for nanoparticle synthesis, their complexity and environmental impact have led to an increasing interest in green synthesis methods (Jamkhande et al., 2019). Green synthesis, mainly using plant-based materials, has gained prominence for its simplicity, cost-effectiveness, and ability to produce crystalline nanoparticles with various shapes and sizes (Vinayagam et al., 2024; Wang et al., 2014b). Various techniques are used for the preparation of IONPs, among which the hydrothermal method stands out for its flexibility in adjusting processing parameters. This method allows the synthesis of nanostructures with different dimensions, including 1D, 2D, and 3D structures (Tadic et al., 2019). Iron oxide nanoparticles exhibit superior chemical stability, low toxicity, and superparamagnetic behavior, making them valuable for supplementary treatment tools, for example in a very promising cancer treatment known as magnetic hyperthermia (Ali et al., 2016). The eco-friendly green synthesis of iron oxide has gained popularity due to its effectiveness, low cost, non-toxicity, and environmentally friendly nature. Plant-based materials, rich in phenolic compounds, act as reducing agents for metal salts, resulting in the production of nanoparticles with unique properties (Jeetkar et al., 2022). Biosynthesis, utilizing microorganisms and plant extracts, has emerged as green and beneficial. Thus, plant-based methods offer advantages such as reduced reaction times and elimination of the cell culture step (Rana et al., 2020). Despite advancements in metal nanoparticle research, a gap exists in sustainable synthesis methods for iron oxide nanoparticles using agricultural waste. Traditional methods are often complex and environmentally impactful. Therefore, there is a need for eco-friendly alternatives. Agro-wastes offer abundant bioactive compounds that can serve as both bioreducing and capping agents. However, further research is needed to fully exploit their potential, as current green methods predominantly rely on high-quality fruits, which can be unprofitable due to their high consumption and consequent loss of nutritional value. This study pioneers a

novel approach by utilizing bioactive compounds from Honduran banana peels for iron oxide nanoparticle synthesis, addressing this gap and promoting sustainability (Aswathi et al., 2023).

Simultaneously, the escalating global plastic crisis has resulted in severe environmental repercussions, with plastic waste polluting oceans, harming wildlife, and contributing to long-lasting ecological damage (Kibria et al., 2023). Conventional plastics, primarily derived from non-renewable fossil fuels, pose a significant challenge due to their non-biodegradable nature (Khoo et al., 2010). In response to these pressing issues, the demand for sustainable alternatives is on the rise. Bioplastics, derived from natural sources such as plant-based materials, offer a promising solution. Unlike traditional plastics, bioplastics have the advantage of being biodegradable and, in some cases, compostable (Cruz et al., 2022; Sharmiladevi et al., 2019).

The production of bioplastics encompasses the use of renewable resources, including corn starch (Zounggran et al., 2020), potato starch (Momotaz et al., 2022), sugarcane (Koller et al., 2009), wheat (Patni et al., 2014), and soybeans (Rahman et al., 2023), as well as specific bioplastics like PLA derived from corn or sugarcane, and innovative sources such as algae (Onen Cinar et al., 2020), hemp (Modi et al., 2018), and wood pulp cellulose (Konwar et al., 2020). These resources not only contribute to mitigating environmental impacts but also reduce dependence on finite fossil fuel reserves. (Cruz et al., 2022). This shift towards bioplastics represents a crucial step in fostering a more environmentally conscious and sustainable approach to material usage. Banana-based biopolymers, with their diverse chemical compositions including proteins, polysaccharides, lipids, ashes, etc., are suitable candidates for developing bioplastics for nano-packagings (Castro-Criado et al., 2023; Phothisarattana et al., 2021).

The novelty of the present research lies in its innovative approach, utilizing agro-waste from Honduran banana peels for the synthesis of iron oxide nanomaterials. This unique methodology takes advantage of the rich availability of bioactive compounds in this kind of agro-waste, which can serve as effective agents in the synthesis process. Therefore, the study aims to contribute to the field of food nano-packaging by offering sustainable and environmentally friendly materials, with a specific focus on the development of bioplastic-based nano-packaging solutions. The results obtained from this research are anticipated to have a substantial impact, introducing new possibilities for the development of more sustainable materials in the field of food preservation and packaging.

The research introduces a pioneering method for recycling common agricultural waste such as banana peel and synthesizing magnetic iron oxide nanoparticles (BPEX-MIONPs) using banana peel extract.

The study focuses on converting banana peels into useful nanomaterials with antioxidant capacity, enabling the development of bioplastics with potential for food preservation, and thus contributing to environmental conservation and bioeconomy. Employing advanced techniques such as X-ray diffraction, transmission electron microscopy, scanning electron microscopy, and Fourier transform infrared spectroscopy, the investigation provides a comprehensive understanding of the magnetite structure and various morphologies of BPEX-MIONPs. This research enhances our knowledge of novel nanocomposites, opening up exciting possibilities for sustainable food preservation and packaging applications in the expanding field of nanotechnology.

## Materials and Methodology

### Materials

The main reagents employed in this study were 98% iron (III) chloride hexahydrate ( $\text{FeCl}_3 \cdot 6\text{H}_2\text{O}$ ), ethanol, NaOH, gallic acid ( $\text{C}_7\text{H}_6\text{O}_5$ ), and 2,2-diphenyl-1-picrylhydrazyl (DPPH). All other chemicals and reagents used were of analytical grade.

Fresh agro-waste banana peels and grapes were supplied from a local market in Danli Honduras.

### Banana Peel Extract Preparation

In the initial phase of our experimental procedure, we focused on the meticulous preparation of banana peel extract for subsequent nanoparticle synthesis. Fresh agro-waste banana peels, selected with care and free from damage, were meticulously washed to remove any potential physical contaminants. The peels were manually removed, cut into smaller pieces, and evenly spread on stainless steel trays. After a 24-hour drying process at a constant temperature of 90 °C, the peel pieces were ground into a finely powdered form using a manual mill. The material underwent additional processing to attain the desired particle sizes of 250–63  $\mu\text{m}$  using a standard test sieve. Following this, maceration extraction was employed, where 50 g of fruit powder was dissolved in 100 mL of water at room temperature ( $25 \pm 2$  °C) for 24 h. After filtration, the concentration of the extract in g/mL was determined.

### BPEX-MIONPs Synthesis

Following the successful extraction of banana peel powder, our focus shifted to synthesizing magnetic iron oxide nanoparticles (BPEX-MIONPs) in the second stage. Essential reagents, a 1 M solution of  $\text{FeCl}_3 \cdot 6\text{H}_2\text{O}$ , and a 5 M solution of NaOH were prepared. The synthesis was initiated by mixing

100 mL of fruit extract with 100 mL of the  $\text{FeCl}_3 \cdot 6\text{H}_2\text{O}$  solution, stirred with a magnetic stirrer. pH adjustment to 7.5 using NaOH (5 M) was crucial. The mixture underwent a 3-hour reaction within the temperature range of 60–80 °C, followed by subsequent steps, including cooling, filtration, washing, and drying of the resulting iron oxide nanoparticles. These nanoparticles were then subjected to pretreatment at 200 °C for 6 h using a laboratory oven. The oven utilizes airflow to facilitate intense heat transmission, aiding in heating, drying (removal of substantial water content from samples), hardening, and sterilizing both materials and chemical salts (Abdullah et al., 2023d). Finally, the nanoparticles underwent a final treatment at 300 °C for 2 h using a muffle furnace (Abdullah et al., 2023c). This furnace is designed to achieve exceptionally high temperatures and employs radiation for continuous heat transfer, thereby facilitating the processing of materials and the combustion of organic substances to eliminate impurities. The process of extraction and synthesis is depicted in Fig. 1, which serves as a schematic design for the experiment.

### BPEX-MIONPs Characterization

In this section, the various methods employed to characterize the nanoparticles were detailed. Our approach involves utilizing X-ray diffraction (XRD) and transmission electron microscopy (TEM). For XRD analysis, patterns were obtained (measured on a Bruker D8 Advance A25 diffractometer with a Cu anode) to confirm the crystalline phase and crystal systems, allowing for the calculation of size and crystallinity of the BPEX-MIONPs, as outlined in a previous study (Abdullah et al., 2023a). Diffractograms were generated within the  $2\theta$  range of 15–70 degrees. The morphology and particle size of BPEX-MIONPs were analyzed using a Zeiss EVO scanning electron microscope for scanning electron microscopy (SEM). Further analysis of nanoparticle morphology and size was performed through TEM using a Talos S200 microscope (FEI, USA) operating at 200 kV. Additionally, Fourier transform infrared spectroscopy (FTIR) was employed to glean insights into the structure of the BPEX-MIONPs by examining vibrational modes in the range of 4000 to 400  $\text{cm}^{-1}$ .

### Antioxidant Activity

During the preparation of banana peel extract (BPEX) and banana peel extract-based magnetic iron oxide nanoparticles (BPEX-MIONPs), an assessment of their antioxidant capacity was conducted using the Disc Diffusion technique against the DPPH free radical (Abdullah et al., 2023c). In this approach, approximately 7 mg of DPPH was dissolved in ethanol, and a 25 mL DPPH free radical solution was spread onto a 10 cm diameter aluminum plate. Subsequently, 0.5

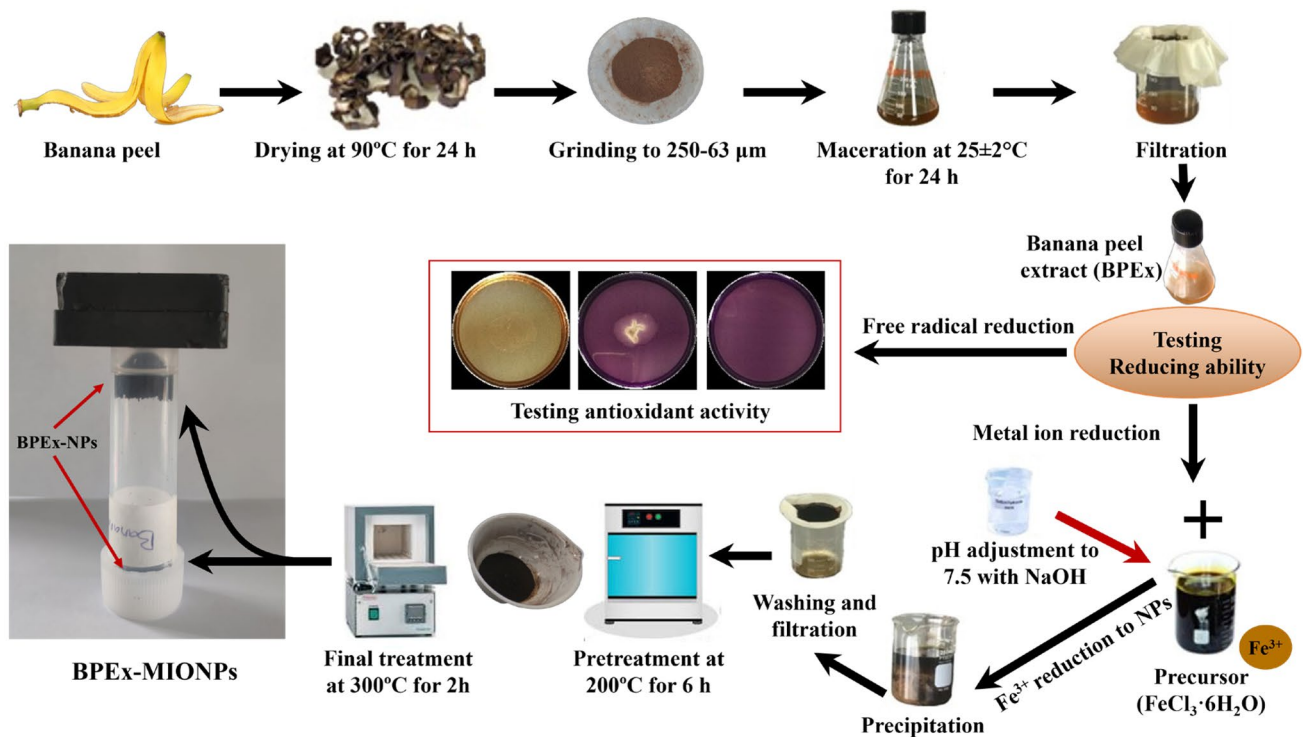


**Fig. 1** Schematic design illustrating the steps involved in the experiment, including the extraction process of banana peel extract (BPEX), testing its ability to reduce free radicals, and its feasibility in reducing iron ions to magnetic nanoparticles (BPEX-MIONPs)

mL of the respective extracts (BPEX and BPEX-MIONPs) was applied at the center of the plate containing the DPPH solution, resulting in an immediate color change to clear yellow. The evaluation of antioxidant activity involved measuring the areas of color change using ImageJ software. The assessment method, validated by recording the area, utilized the formula for inhibition percentage:

$$\text{Inhibition (\%)} = \left( \frac{\text{Zone}_1 - \text{Zone}_2}{\text{Zone}_1} \right) \times 100 \quad (1)$$

where  $\text{Zone}_1$  represents the total area of inhibited DPPH with violet color, and  $\text{Zone}_2$  represents the remaining areas without a change in color over time. A complete color change to yellow is recorded as 100% inhibition. This technique serves as a valuable tool for quantifying the antioxidant capacity of BPEX and BPEX-MIONPs, providing crucial insights into their potential applications, including in the synthesis of iron oxide nanoparticles.

### Bioplastic Solution Preparation

Based on the results of a previous study (Castro-Criado et al., 2023), banana agro-waste from Mesa SAN R11 El Paraíso, Honduras, was subjected to a meticulous process to transform it into flour. After peeling and slicing, the

material was dried, tempered, and milled to achieve the desired characteristics. The presented protocol revealed banana composition: moisture (1.50%), ashes (7.81%), lipids (0.22%), proteins (2.25%), and polysaccharides (59.2%). An aqueous banana water solution (1–3) was prepared, where 1 gram dissolved in 30 mL of water, followed by stirring for approximately 10 min at 100 °C. After filtration using coffee filtration paper, the resulting solution was collected as the liquid, and approximately 7 mg of glycerin was thoroughly mixed in to form the bioplastic (Abdullah et al., 2022).

### Dip Coating of Grapes

Given the nutrient-rich composition of grapes and their susceptibility to microbial decay, we selected them to assess the feasibility of using BPEX-MIONPs stabilized with banana-based bioplastic as a bio-coating for food nanopackaging. Approximately 7 mg of BPEX-MIONPs were introduced into the solution forming the bioplastic, and manually mixed with the banana solution until a visually homogeneous dispersion was achieved. Subsequently, grapes were immersed in the resulting solutions—both with and without BPEX-MIONPs—for 3 min. The samples were then left at room temperature ( $28 \pm 7$  °C) with an average relative humidity (RH) of  $\approx 87\%$  for a 6-day shelf-life test. At three-day intervals, images were

captured, and the weight loss rate (WLR, %) was calculated as follows (Mohammed et al., 2023):

$$\text{WLR}(\%) = \left( \frac{P_{\text{Fresh}} - P}{P_{\text{Fresh}}} \right) \times 100 \quad (2)$$

where  $P_{\text{Fresh}}$  and  $P$  are the weights of fresh and preserved grapes, respectively.

### Statistical Analysis

Measurements from three replicates were subjected to one-way ANOVA to identify significant differences using OriginLab software.

## Results and Discussion

### Crystallographic Insights (XRD)

The XRD results for banana peel extract-based magnetic iron oxide nanoparticles (BPEX-MIONPs) are illustrated in Fig. 2. Prominent peaks are discernible at  $18.42^\circ$ ,  $21.29^\circ$ ,  $23.85^\circ$ ,  $26.16^\circ$ ,  $26.19^\circ$ ,  $30.29^\circ$ ,  $30.32^\circ$ ,  $33.97^\circ$ ,  $43.36^\circ$ ,  $47.49^\circ$ , and  $53.83^\circ$ , corresponding to crystallographic planes (hkl) (1 1 1), (2 0 0), (2 0 1), (2 1 1), (1 1 2), (2 2 0), (2 0 2), (3 0 1), (4 0 0), (3 3 1), and (4 2 2), respectively. These peaks are identified as maghemite ( $\text{Fe}_2\text{O}_3$ ), exhibiting a calculated pattern quality of C. The crystal system is tetragonal, characterized by the space group P 43 21 2, according

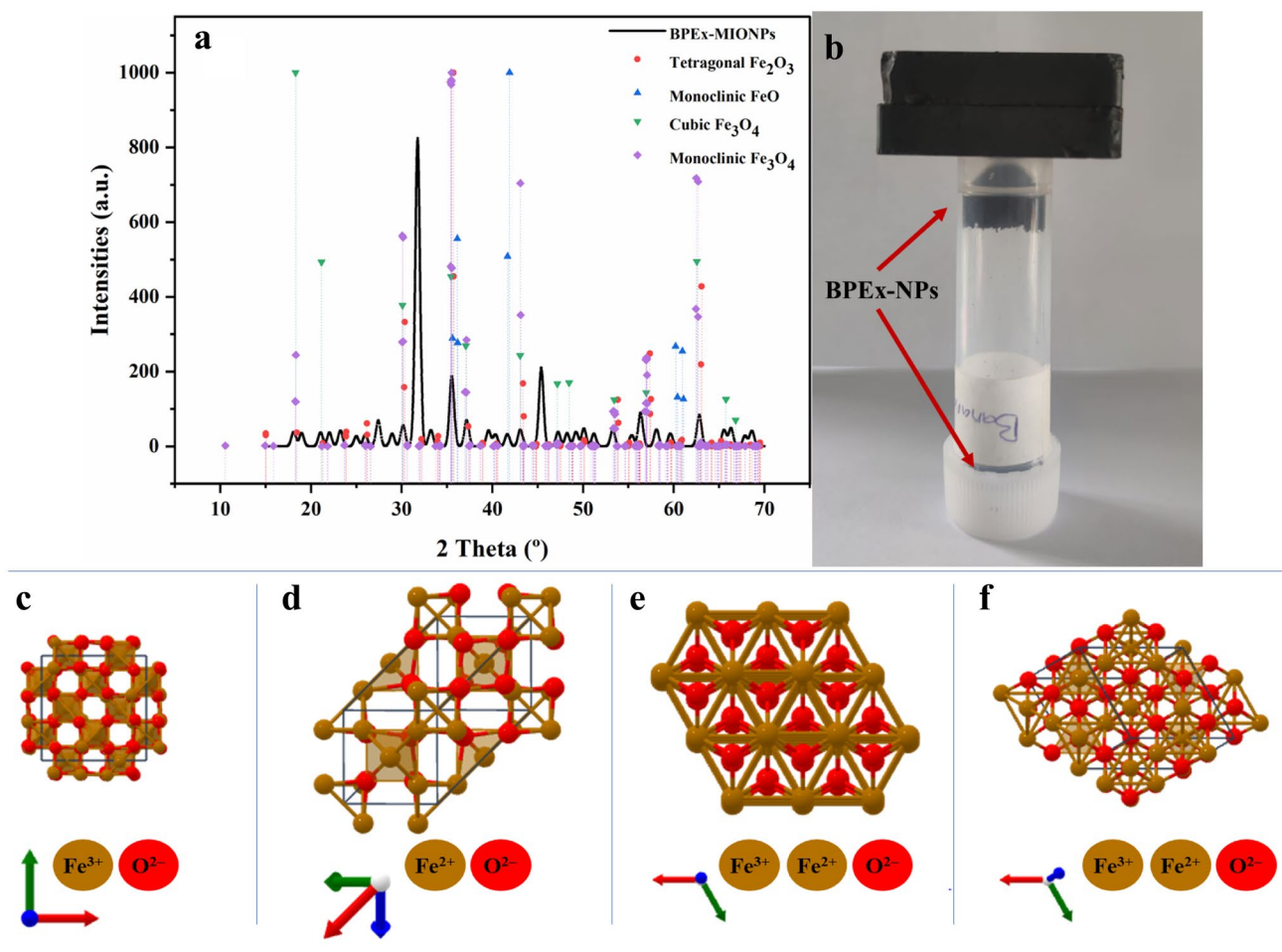


**Fig. 2** XRD results for BPEX-MIONPs, displaying crystallographic peaks of  $\text{Fe}_2\text{O}_3$ ,  $\text{Fe}_3\text{O}_4$ , and  $\text{FeO}$  (a), accompanied by visual representations of their magnetic responses (b). The model structure obtained from the XRD analysis reveals the crystallographic behavior

of BPEX-MIONPs, emphasizing distinct phases, including tetragonal  $\text{Fe}_2\text{O}_3$  (c), monoclinic  $\text{FeO}$  (d), cubic  $\text{Fe}_3\text{O}_4$  (e), and monoclinic  $\text{Fe}_3\text{O}_4$  (f)

to the reference code 00-901-2692, as reported by Greaves (Greaves, 1983).

Similarly, diffraction peaks at 35.60°, 36.13°, 36.17°, 41.68°, 41.89°, 60.19°, 60.40°, 60.95°, and 61.06°, corresponding to crystallographic planes (hkl) (0 0 1), (1 1 0), (2 0–1), (2 0 0), (1 1–1), (1 1 1), (2 0–2), (3 1–1), and (0 2 0), respectively, are attributed to wuestite (FeO). The crystal structure demonstrates a monoclinic system with the space group C12/m1, as reported in (Fjellvag et al., 2002) (Reference Code: 00-900-2670).

Furthermore, distinct diffraction peaks at 18.29°, 21.15°, 30.09°, 35.44°, 37.0692°, 43.07°, 47.16°, 48.46°, 53.43°, 56.96°, 62.54°, 65.76°, 66.82°, and 68.8° corresponding to crystallographic planes (hkl) (1 1 1), (2 0 0), (2 2 0), (3 1 1), (2 2 2), (4 0 0), (3 3 1), (4 2 0), (4 2 2), (5 1 1), (4 4 0), (5 3 1), (4 4 2) [F-4 3 m (216)], and (442) [Fd-3 m:2 (227)], respectively, are attributed to Fe<sub>3</sub>O<sub>4</sub>. This material exhibits a cubic crystal system with a space group of F-43 m, as reported by (Fleet, 1986) (Reference Code: 00-153-9747). The crystallographic parameters include a lattice parameter of  $a = 8.3941 \text{ \AA}$ , resulting in a cell volume of  $591.46 \text{ \AA}^3$ . The crystal structure is characterized by a face-centered cubic arrangement with a unit cell containing 8 formula units ( $Z = 8$ ). The X-ray wavelength used for diffraction analysis is  $1.54056 \text{ \AA}$ , with a copper K $\alpha$  source having a  $\mu(\text{Cu K}\alpha)$  of  $1151.001 \text{ cm}^{-1}$ .

The calculated crystallinity index is 99.9%, highlighting the high degree of crystallinity in the synthesized nanoparticles. Individual peaks exhibit varying crystallinity percentages, with the peak at 31.68° (202) corresponding to monoclinic Fe<sub>3</sub>O<sub>4</sub> (Wright et al., 2002) (Reference Code: 00-153-2800), demonstrating 10.4% crystallinity. These results confirm the well-defined crystalline structure of BPEX-MIONPs, providing essential insights into their physical and chemical properties in the context of agro-waste-based nanoparticle synthesis.

The degree of crystallinity, reflecting the structural organization in a material's crystalline state, is instrumental in quantifying oxidation phases across different phases. This determination entails calculating the ratio of the area under crystalline peaks in the XRD pattern to the total area under all peaks in the pattern. Furthermore, phase quantification can be mathematically derived from this ratio using the following equation (Abdullah et al., 2023a):

$$\text{Crystallinity degree (\%)} = \frac{\text{The area under crystalline peaks}}{\text{Total area under all peaks}} \times 100 \quad (3)$$

The average crystalline size, calculated using the Debye-Scherrer formula, is determined to be 14.8 nm. Magnetic responses of these structures are depicted in Fig. 2b, illustrating the correlation between the different systems and their magnetic behavior.

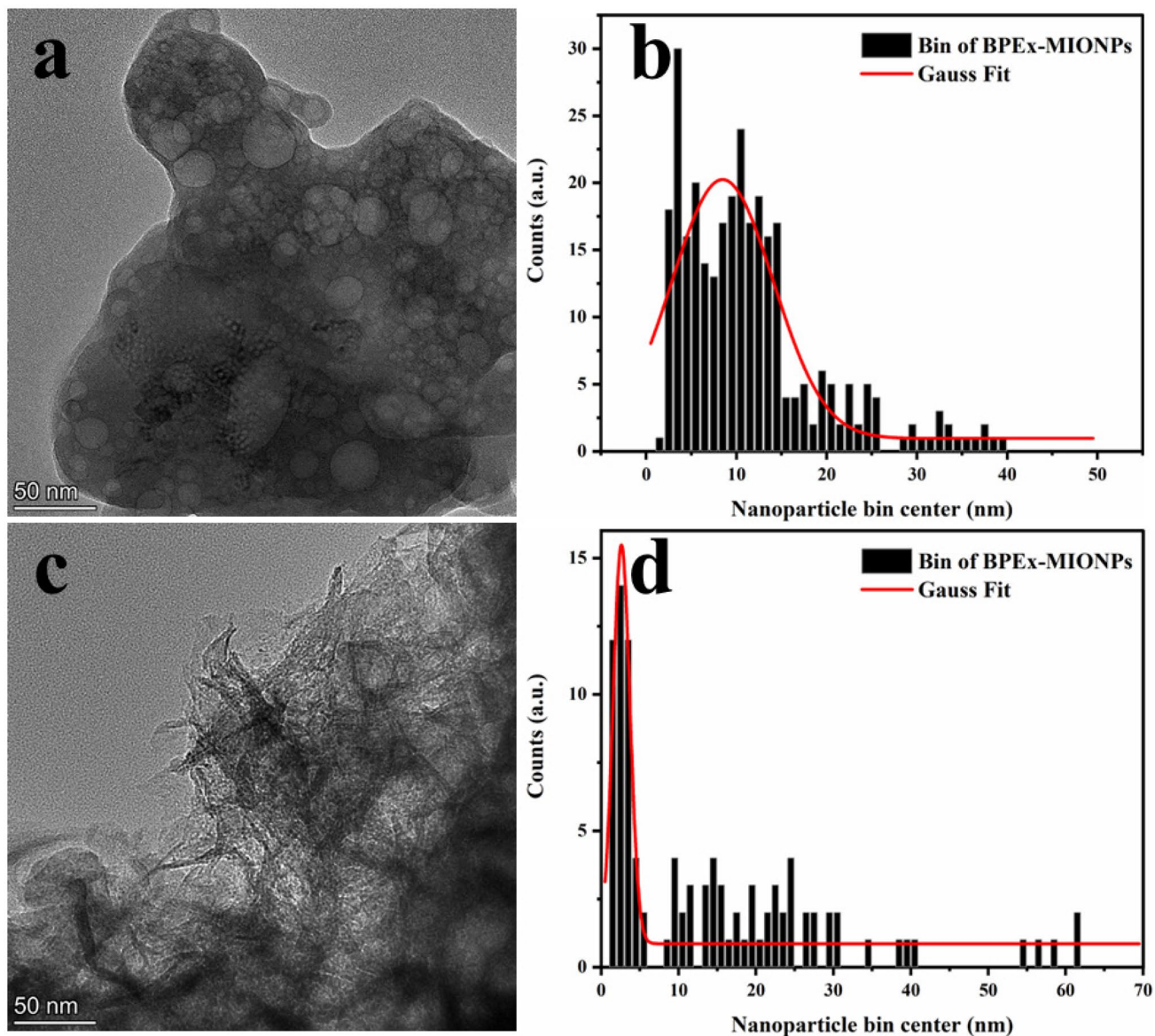
## Nanoparticle Visualization (TEM)

Figure 3 illustrates the TEM analysis of BPEX-MIONPs, revealing a diverse array of morphologies, including both spherical and elongated nanoparticles (thin fibrillar). In Fig. 3a, distinctive spherical shapes ranging from 5 to 39 nm, with an average diameter distribution of  $8.5 \pm 0.6 \text{ nm}$ , are evident, as depicted in Fig. 3b. These spherical nanoparticles hold significant promise for applications in fields such as medicine, electronics, and nanotechnology owing to their compact form and magnetic properties (Park et al., 2018).

In contrast, Fig. 3c reveals nanoparticles with varying thickness along their length, displaying thin fibrillar shapes ranging from ultrafine nanofibrils to elongated nanorods (referred to as variable-edge nanorods). These nanoparticles exhibit diameters ranging from 1 to 62 nm, with a total average diameter distribution of  $2.6 \pm 0.1 \text{ nm}$  (Fig. 3d). These nanofibrils exhibit unique characteristics, such as a larger surface area and a more robust interaction with their environment. Consequently, they emerge as potentially intriguing candidates for applications in sensors, catalysts, and optoelectronic devices (Avolio et al., 2019). It is crucial to note that the size and shape of nanoparticles or nanofibrils play a pivotal role in influencing their properties and behavior. While the average diameter serves as a valuable metric for characterizing the size of nanoparticles within a sample, the consideration of size distribution is equally essential. This distribution can vary, ranging from highly uniform nanoparticles/nanofibrils to those with more dispersed sizes. Similar spherical morphologies have been reported in (Simol et al., 2020; Venkateswarlu et al., 2014), and elongated shapes have been reported in (Avolio et al., 2019).

## SEM

Figure 4 provides an image of the intricate particle assembly of the synthesized BPEX-MIONPs, displaying an interplay of shapes and structures. SEM image shows an array predominantly made up of spherical nanoparticles, which resemble coral reef formations (Fig. 4a). The nanoparticle assemblies presented in this study emulate the collaborative dynamics observed in coral reefs, wherein colonies of particles intricately coalesce through a synergistic interaction between phytochemicals and magnetic ions, giving rise to agglomerates and aggregates. SEM images were meticulously processed using the ImageJ software's image calculator, incorporating thresholding and Gaussian blur filters (Abdullah et al., 2023b). The analyzed particles were subjected to Gauss fit analysis using OriginLab, revealing a nanoparticle diameter of  $7.9 \pm 1.5 \text{ nm}$ , as illustrated in Fig. 4b. Notably, this size aligns well with findings from XRD (14.8 nm) and TEM (8.5 nm for the spherical shapes, and 2.6 for the ultrafine nanofibrils),



**Fig. 3** TEM analysis of BPEX-MIONPs displays diverse morphologies, including spherical nanoparticles (a) with their average diameter distribution (b), and nanofibrillar shapes (c) with their average diameter distribution (d)

with minor discrepancies attributed to variations in each technique's setup (Tuoriniemi et al., 2014). The observed variations between the techniques could arise from several factors, including differences in sample preparation, instrument calibration, and measurement methodologies. XRD provides an average particle size based on diffraction patterns, while TEM offers direct visualization of individual nanoparticles. However, it's important to note that XRD measures the crystal lattice size, which may differ from the actual nanoparticle size due to factors such as crystal defects or strain. Additionally, TEM measurements might be influenced by factors like sample preparation techniques, staining methods, and the potential for particle

aggregation. Despite these minor discrepancies, the consistency among the techniques reinforces the robustness of our nanoparticle size determination. Integrating data from multiple techniques enhances the reliability of our findings and provides a comprehensive understanding of the nanoparticles' morphology and size distribution.

Moreover, the SEM particle agglomerate size distribution, depicted in Fig. 4c, unveils a diverse range spanning from 10 to 1200 nm, with an average size of approximately 487.9 nm. This broad distribution underscores the versatility in particle sizes within the assembly, encompassing smaller individual nanoparticles to larger agglomerates. The observed range signifies a well-defined and controlled

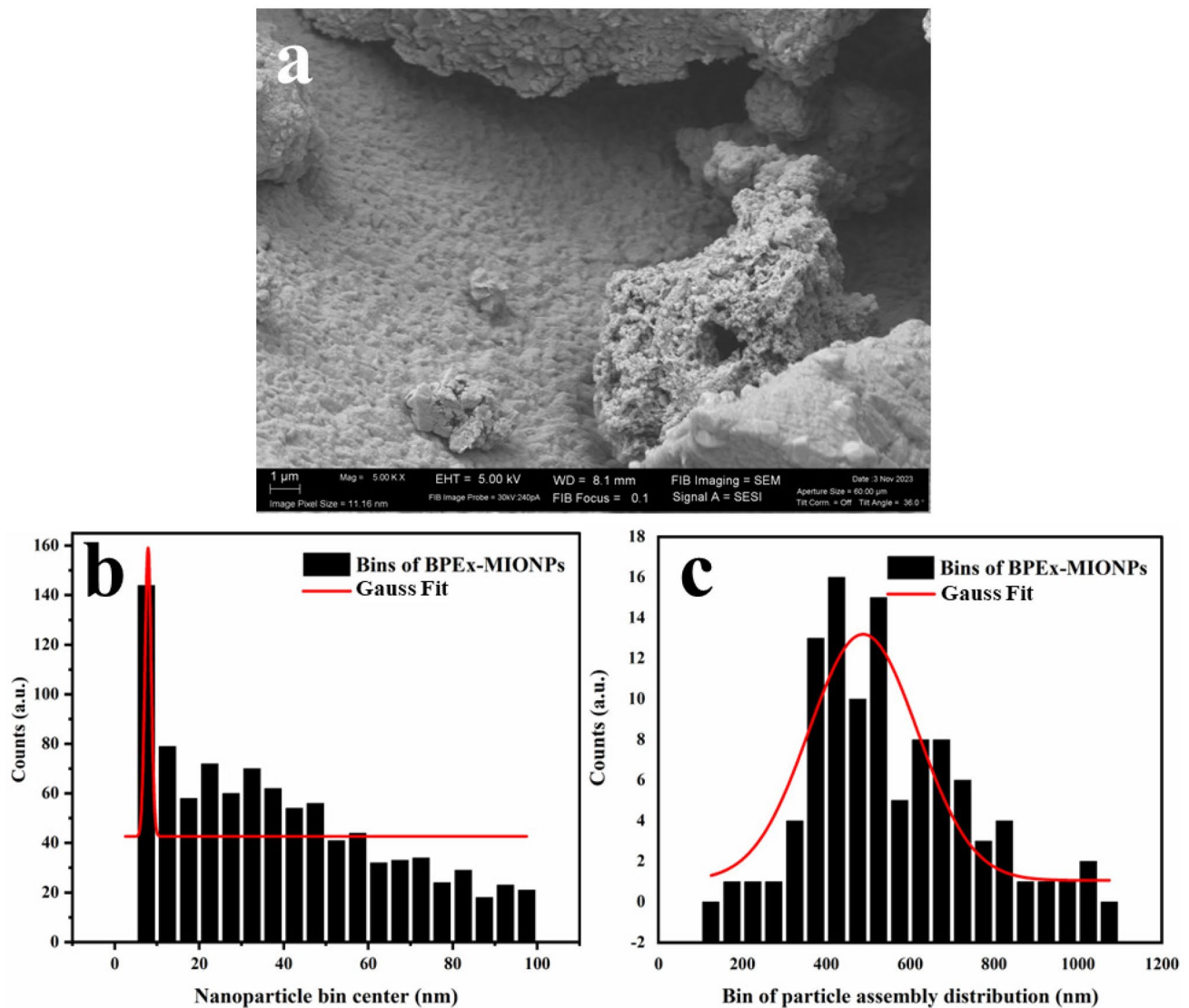


**Fig. 4** SEM images depicting the coral reef-like assembly of BPEX-MIONPs, formed by spherical nanoparticles (a). Nanoparticle diameter distribution, calculated by Gaussian fitting and ranging from 0 to

100 nm, with an average size of ca. 7.9 nm (b). Size distribution of particle assembly (agglomerates), ranging from 10 to 1200 nm, with an average size of ca. 487.9 nm (c)

synthesis process, enabling the formation of nanoparticles with varied sizes and configurations.

Comparing our morphological aspects with iron oxide prepared using different methods, our study stands out as the first to achieve well-defined forms and smaller sizes. For instance, Üstün (2021) utilized *Ficus Carica* Leaf Extract and obtained iron oxide nanoparticles with agglomeration and multiform shapes ranging in size from 43 to 57 nm (Üstün, 2021). Juby et al. (2022) obtained porous and irregularly shaped iron oxide nanoparticles with rough surfaces using *Simarouba Glauca* Leaf Extract, demonstrating sizes ranging from 70 to 122 nm (Juby et al., 2022). Similarly, cube-shaped iron oxide nanoparticles were obtained using *Lagenaria Siceraria*, with an average size ranging from 30 to

100 nm (Kanagasubbulakshmi & Kadirvelu, 2017). Furthermore, Kang et al. (2023) employed the solvothermal method to produce magnetic  $\text{Fe}_3\text{O}_4$  and modified it with phytic acid (PA). Interestingly, the  $\text{Fe}_3\text{O}_4$  exhibited an irregular spherical shape and a slightly rough surface, with minimal morphological changes observed upon functionalization with PA. Additionally, aggregation decreased from 510 to 310 nm with PA, suggesting that incorporating more organophosphate compounds of natural origin could further enhance properties (Kang et al., 2023).

The distinctive coral reef-like assembly observed in Fig. 4a not only highlights the innovative synthesis approach but also underscores the potential applications of these BPEX-MIONPs. The combination of unique shapes, sizes,



and magnetic properties enhances their adaptability for various uses, from biomedical applications to environmental remediation (Fahmy et al., 2018). This intricate particle assembly contributes to the overall understanding of the synthesized nanoparticles, emphasizing their potential as multifunctional materials with diverse applications.

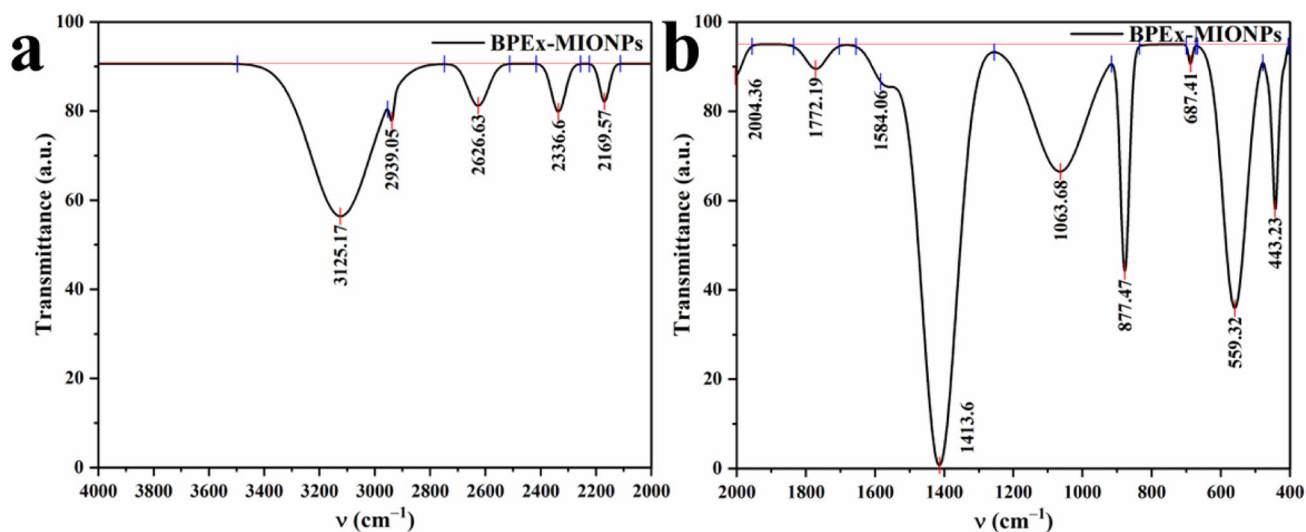
### Chemical Signature (FTIR)

As can be seen in Fig. 5, the FTIR spectrum of the synthesized magnetic iron oxide nanoparticles using banana peel extract (BPEX-MIONPs) reveals a rich tapestry of functional groups contributing to their physicochemical properties. The prominent band at 3465  $\text{cm}^{-1}$ - 3000  $\text{cm}^{-1}$  in Fig. 5. signifies O-H stretching vibrations, indicative of hydroxyl groups, possibly originating from water molecules or hydroxyl molecules linked by hydrogen bonds (Rajeswari et al., 2021; Salgado et al., 2019). The absorption band observed at 2939.1  $\text{cm}^{-1}$  signifies the symmetric stretching vibrations attributed to aliphatic hydrocarbons (CH) and methylene ( $-\text{CH}_2$ ) groups, which are frequently encountered in organic compounds (Wang et al., 2014a). The presence of  $\text{C}\equiv\text{C}$  stretching vibrations at 2626.6  $\text{cm}^{-1}$  (Fig. 5a) suggests the involvement of alkynes or acetylene groups (Cefali et al., 2015; Chandrasekar et al., 2013). Additionally, the peak at 2336.6  $\text{cm}^{-1}$  (Fig. 5a) could be attributed to the presence of carbon dioxide ( $\text{CO}_2$ ) during analysis. The peak at 2169.6  $\text{cm}^{-1}$  (Fig. 5a) may indicate the presence of cyanide groups (CN), suggesting nitrogen-containing compounds. Moving to the lower wavenumber range in Fig. 5b, the peaks at 2004.4  $\text{cm}^{-1}$  and 1772.2  $\text{cm}^{-1}$  are characteristic of  $\text{C}=\text{O}$  stretching vibrations, with the former possibly associated

with ketones or aldehydes and the latter suggesting ester groups (Rajeswari et al., 2021). The peak at 1584.1  $\text{cm}^{-1}$  corresponds to  $\text{C}=\text{C}$  stretching vibrations, indicative of unsaturated carbon-carbon bonds (Salgado et al., 2019). Further analysis in Fig. 5b reveals the presence of methylene ( $\text{CH}_2$ ) bending vibrations at 1413.6  $\text{cm}^{-1}$ , while the peak at 1211  $\text{cm}^{-1}$  suggests C-O stretching vibrations, characteristic of ether groups or alcoholic functionalities (Nalbandian et al., 2015; Zhang et al., 2011). The absorption peak around 1063.7  $\text{cm}^{-1}$  is associated with C-O, C-O-C, and C-O-H stretching vibrations, suggesting the presence of polysaccharides functional or groups phenolic compounds ( $-\text{OH}$ ) (Nandiyanto et al., 2019; Salgado et al., 2019). Finally, the peaks at 877.5  $\text{cm}^{-1}$ , 773.3  $\text{cm}^{-1}$ , and 687.4  $\text{cm}^{-1}$  in Fig. 5b are attributed to metal-oxygen (Fe-O) stretching vibrations, confirming the presence of iron oxide ( $\text{Fe}_3\text{O}_4$ ) in the synthesized nanoparticles (Nalbandian et al., 2015; Zhang et al., 2011). The peaks at 559.3  $\text{cm}^{-1}$  and 443.2  $\text{cm}^{-1}$  in Fig. 5b indicate metal-oxygen (Fe-O) bending vibrations ( $\alpha\text{-Fe}_2\text{O}_3$ ), further supporting the identification of iron oxide (Manzo et al., 2020). This intricate network of functional groups signifies the complex composition of BPEX-MIONPs, showcasing the diverse interactions contributing to the stabilization and functionalization of these magnetic nanoparticles.



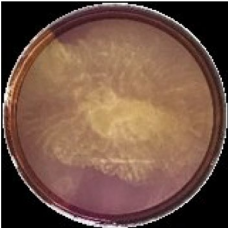


### Assessing Antioxidant Properties

The evaluation of antioxidant activity in banana peel extract (BPEX) through the DPPH free radical assay demonstrated remarkable results, as outlined in Table 1. The initial inhibition, starting at 9.89% after 5 s (T2), progressively increased, reaching 65.61% at 6 min (T3), 89.98% at 12 min (T4),



**Fig. 5** FTIR spectra (3500–2000  $\text{cm}^{-1}$ ) of BPEX-MIONPs reveal diverse functional groups, including hydroxyls and carbonyls (a) and lower wavenumber range (2000–400  $\text{cm}^{-1}$ ) highlights metal-oxygen bonds, contributing to the comprehensive chemical characterization (b)

**Table 1** Antioxidant activity of banana peel extract (BPEx) over time in the DPPH free radical assay confirmed by visualized photographs depicting color change

T1 = 0 s	T2 = 5 s	T3 = 6 min	T4 = 12 min	T5 = 18 min
				
0%	9.9%	65.6%	90%	100%

and ultimately achieving a complete inhibition of 100% at 18 min (T5). This temporal trend signifies the dynamic enhancement of antioxidant properties within the banana extract over the assessment period. The outstanding antioxidant properties of the banana peel extract were further evidenced by a noticeable color change during the DPPH free radical assay. The extract exhibited an initial yellow hue, intensifying to a clearer yellow over time, as evidenced by the color change, indicating an increase in the inhibition percentage, as can be seen in Table 1. This distinct color transformation, correlated with the temporal progression of the assay, aligns with the concurrent increase in inhibition percentage, as illustrated in Table 1. The dynamic shift in color serves as a visual confirmation of the escalating antioxidant activity, providing additional support to the quantitative results obtained through the DPPH assay.

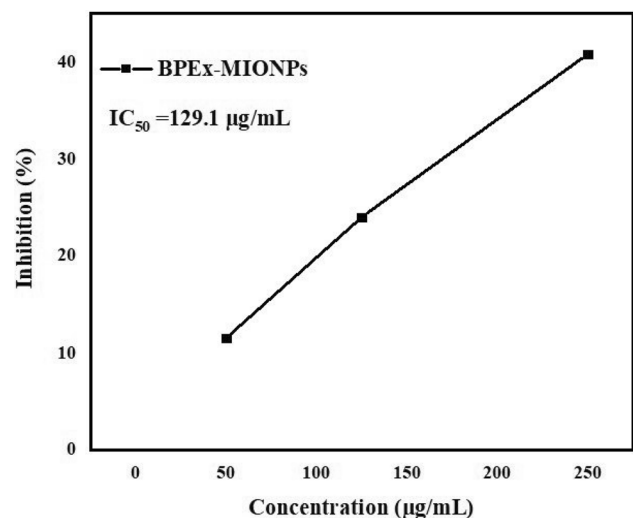
Banana peels boast robust antioxidant properties, primarily attributed to polyphenolic compounds like catechins, epicatechins, and gallic acid. Flavonoids such as quercetin and rutin, along with tannins, amplify the antioxidant and other capabilities. The presence of dopamine, dietary fiber, vitamins (especially vitamin C), and carotenoids like beta-carotene further enhances these health-promoting qualities (Cefali et al., 2015; Islam et al., 2023; Salgado et al., 2019).

The assessment of antioxidant activity in BPEx-MIONPs, as revealed by the  $IC_{50}$  value of 129.1  $\mu\text{g}/\text{mL}$  (Fig. 6), underscores the substantial antioxidant potential embedded within these magnetic nanoparticles. This high antioxidant activity can be attributed to the synergistic effects arising from the unique combination of banana phytochemicals and the structural attributes of magnetic ions (Apak et al., 2007; Kanagasubbulakshmi & Kadirvelu, 2017).

The observed size of BPEx-MIONPs, as determined by TEM (approximately from 2.1 to 8.5 nm) and XRD (14.8 nm), is a crucial factor contributing to their enhanced antioxidant capacity. The nanoparticles' nanoscale dimensions amplify their surface area, facilitating increased interactions between the nanoparticles and free radicals, thereby increasing their scavenging capability (Affes et al., 2020). This phenomenon is further supported by the distinct shapes

observed in TEM images, showing both spherical and elongated forms. The diverse morphologies indicate a heterogeneous distribution of particle shapes, potentially leading to varied reactivity toward free radicals (Rajakumar et al., 2018). Moreover, the magnetic ions present in the nanoparticles contribute to their antioxidant activity (Santoyo Salazar et al., 2011). The magnetic properties inherent in the structure of BPEx-MIONPs may facilitate electron transfer reactions, playing a role in the reduction of free radicals and, consequently, enhancing their antioxidant efficacy. This characteristic provides an additional dimension to their antioxidant activity, distinguishing them from conventional antioxidant agents.

The simultaneous presence of banana phytochemicals and magnetic ions creates a multifaceted antioxidant system within BPEx-MIONPs, where the various components act synergistically to efficiently neutralize free radicals (Cartwright et al., 2020). This innovative amalgamation of natural plant-derived compounds and magnetic nanoparticles not only enhances antioxidant capabilities but also holds promise for diverse applications, including fields such as biomedical or

**Fig. 6** Antioxidant activity assessment of BPEx-MIONPs, demonstrating an  $IC_{50}$  value of 129.1  $\mu\text{g}/\text{mL}$

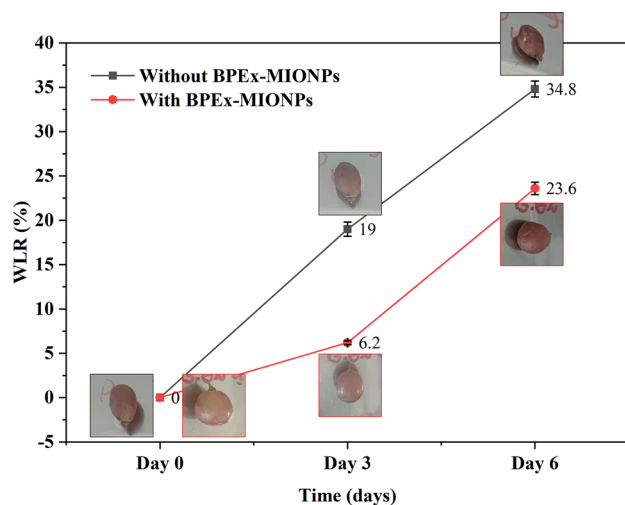


**Fig. 7** Comparative water loss rates (WLR) in grape preservation between control samples and those treated with banana peel extract-based magnetic iron oxide nanoparticles (BPEX-MIONPs)

environmental. The versatility in shape, size, and structural attributes demonstrated by TEM and XRD collectively contribute to the superior antioxidant performance of BPEX-MIONPs, marking them as promising candidates for further exploration in nanotechnology and antioxidant applications.

### Dip Coating of Grapes

In the context of grape preservation with bioplastic coating, our observations in the control group (coated in the absence of BPEX-MIONPs) revealed a significant reduction in water content, with a 19% loss by day 3 and a substantial 34.8% loss by day 6 (Fig. 7). In stark contrast, the grape samples coated with banana peel extract-based magnetic iron oxide nanoparticles (BPEX-MIONPs) exhibited remarkable preservation efficiency, showing only a 6.2% water loss on day 3 and a comparatively lower 23.6% loss on day 6. These findings distinctly demonstrate the superior preservation capacity of the banana nanoparticles in food, emphasizing their potential as a valuable and eco-friendly solution for extending the shelf life of perishable produce (Galus et al., 2020). The controlled release properties and stabilizing effects of BPEX-MIONPs contribute to reducing water loss and maintaining the freshness of preserved grapes over an extended period.

### Conclusions

This study represents a significant step forward in harnessing the potential of agro-waste banana peels for the synthesis of magnetic iron oxide nanoparticles (BPEX-MIONPs), showing

their dual functionality in antioxidant capacity and food preservation. The diverse morphologies revealed through XRD, TEM, and SEM analyses, combined with the confirmation of Fe–O bonds through FTIR, support the successful fabrication of nanoparticles with unique structural characteristics. The robust antioxidant activity observed against DPPH free radicals, along with the preservation efficiency demonstrated in grape storage, underscores the practical applications of BPEX-MIONPs in sustainable food packaging.

Nevertheless, it is crucial to acknowledge certain limitations in our study. While improvements in preservation capacity have been observed, there is a need to enhance laboratory experiments by accounting for variations in humidity, temperature, and other environmental factors. These conditions could have influenced the results, suggesting that an extended shelf life of the preserved food might be achievable under ideal circumstances. Furthermore, the study primarily focused on the characterization of BPEX-MIONPs. Future research should address the imperative need for advanced toxicity studies and *in vivo* evaluations, ensuring the safety and efficacy of these nanoparticles in real-world applications.

Moving forward, refining experimental conditions, incorporating advanced characterization techniques, and expanding the scope to include comprehensive toxicity assessments will be crucial in unlocking the full potential of BPEX-MIONPs. Moreover, exploring broader applications across various contexts will contribute to the development of innovative and sustainable solutions in the fields of nanotechnology and food preservation.

**Acknowledgements** The authors acknowledge the MCI/AEI/FEDER, EU project (Ref. PID2021-124294OB-C21) that supports this work. In addition, the authors thank the CONVOCATORIA DE AYUDAS PARA LA FORMACIÓN EN COOPERACIÓN INTERNACIONAL PARA EL DESARROLLO CON ESTANCIAS EN TERRENO 2022/2023, DE LA OFICINA DE COOPERACIÓN AL DESARROLLO DE LA UNIVERSIDAD DE SEVILLA. J.A.A.A would like to thank the support from the Hayel Saeed Anam group represented by Abdul Jabbar Hayel Saeed Anam. The authors express gratitude to CITIUS for providing access to and assisting with the SEM and TEM area characterization under microscopy services. Additionally, the authors appreciate the support received from CITIUS for FTIR microanalysis services and XRD characterization area.

**Author Contributions** Johar Amin Ahmed Abdullah: Conceptualization, Methodology, Software, Validation, Formal Analysis, Investigation, Resources, Data Curation, Writing—Original Draft Preparation, Writing—Review and Editing, Visualization, Supervision, Funding Acquisition. Silvia Nicole Pérez Lagos: Software, Investigation, Resources, Data Curation, Writing—Original Draft Preparation. Emanuel Josué Estrada Sanchez: Software, Investigation, Resources, Data Curation, Writing—Original Draft Preparation. Octavio Rivera-Flores: Conceptualization, Writing—Review and Editing, Visualization, Project Administration, Funding Acquisition. Marlon Sánchez-Barahona: Conceptualization, Writing—Review and Editing, Visualization, Project Administration, Funding Acquisition. Antonio Guerrero: Conceptualization, Methodology, Validation, Writing—Review and Editing,

Visualization, Supervision, Project Administration, Funding Acquisition. Alberto Romero: Conceptual-ization, Validation, Formal Analysis, Investigation, Resources, Data Curation, Writing—Original Draft Preparation, Writing—Review and Editing, Visualization, Supervision, Project Administration, Funding Acquisition. Note: Silvia Nicole Pérez Lagos and Emanuel Josué Estrada Sanchez contributed equally to this work. All authors have read and agreed to the published version of the manuscript.

**Funding** Funding for open access publishing: Universidad de Sevilla/CBUA This study was financially supported by MICIN/AEI/<https://doi.org/10.13039/501100011033/ERDF/EU>, through the project PID2021-124294OB-C21. International Cooperation Project Ref. 2022/ACDE/000265 funded by the Agencia Española de Cooperación Internacional (AECID).

**Data Availability** Data is provided within the manuscript.

## Declarations

**Institutional Review Board Statement** Not applicable.

**Informed Consent** Not applicable.

**Competing Interests** The authors declare no competing interests.

**Open Access** This article is licensed under a Creative Commons Attribution 4.0 International License, which permits use, sharing, adaptation, distribution and reproduction in any medium or format, as long as you give appropriate credit to the original author(s) and the source, provide a link to the Creative Commons licence, and indicate if changes were made. The images or other third party material in this article are included in the article's Creative Commons licence, unless indicated otherwise in a credit line to the material. If material is not included in the article's Creative Commons licence and your intended use is not permitted by statutory regulation or exceeds the permitted use, you will need to obtain permission directly from the copyright holder. To view a copy of this licence, visit <http://creativecommons.org/licenses/by/4.0/>.

## References

- Abdullah, J. A. A., Díaz-García, Á., Law, J. Y., Romero, A., Franco, V., & Guerrero, A. (2023a). Sustainable nanomagnetism: investigating the influence of green synthesis and pH on iron oxide nanoparticles for enhanced biomedical applications. *Polymers (Basel)*, *15*, 3850. <https://doi.org/10.3390/polym15183850>
- Abdullah, J. A. A., Díaz-García, Á., Law, J. Y., Romero, A., Franco, V., & Guerrero, A. (2023b). Quantifying the structure and properties of nanomagnetic iron oxide particles for enhanced functionality through chemical synthesis. *Nanomaterials*, *13*, 2242. <https://doi.org/10.3390/nano13152242>
- Abdullah, J. A. A., Jiménez-Rosado, M., Guerrero, A., & Romero, A. (2023c). Effect of calcination temperature and time on the synthesis of iron oxide nanoparticles: Green vs chemical method. *Materials (Basel)*, *16*, 1798. <https://doi.org/10.3390/ma16051798>
- Abdullah, J. A. A., Rosado, M. J., Guerrero, A., & Romero, A. (2023d). Eco-friendly synthesis of ZnO-nanoparticles using phoenix dactylifera L., polyphenols: Physicochemical, microstructural, and functional assessment. *New Journal of Chemistry*, *47*, 4409–4417. <https://doi.org/10.1039/D3NJ00131H>
- Abdullah, J. A. A., Salah Eddine, L., Abderrhmane, B., Alonso-González, M., Guerrero, A., & Romero, A. (2020). Green synthesis and characterization of iron oxide nanoparticles by phoenix dactylifera leaf extract and evaluation of their antioxidant activity. *Sustain Chem Pharm*, *17*, 100280. <https://doi.org/10.1016/j.scp.2020.100280>
- Abdullah, J. A. A., Yemişken, E., Guerrero, A., & Romero, A. (2022). Marine collagen-based antibacterial film reinforced with graphene and iron oxide nanoparticles. *International Journal of Molecular Sciences*, *24*, 648. <https://doi.org/10.3390/ijms24010648>
- Affes, S., Maalej, H., Aranaz, I., Kchaou, H., Acosta, N., Heras, Á., Nasri, M., Sawsan, A., Maalej, H., Aranaz, I., Kchaou, H., Acosta, N., Heras, Á., & Nasri, M. (2020). Controlled size green synthesis of bioactive silver nanoparticles assisted by chitosan and its derivatives and their application in biofilm preparation. *Carbohydrate Polymers*. <https://doi.org/10.1016/j.carbpol.2020.116063>
- Ali, A., Zafar, H., Zia, M., ul Haq, I., Phull, A. R., Ali, J. S., & Husain, A. (2016). Synthesis, characterization, applications, and challenges of iron oxide nanoparticles. *Nanotechnology, Science and Applications*, *9*, 49–67. <https://doi.org/10.2147/NSA.S99986>
- Apak, R., Güçlü, K., Demirata, B., Özyürek, M., Çelik, S. E., Bektaşoğlu, B., Berker, K. I., & Özyurt, D. (2007). Comparative evaluation of various total antioxidant capacity assays applied to phenolic compounds with the CUPRAC assay. *Molecules*, *12*, 1496–1547. <https://doi.org/10.3390/12071496>
- Aswathi, V. P., Meera, S., Maria, C. G. A., & Nidhin, M. (2023). Green synthesis of nanoparticles from biodegradable waste extracts and their applications: A critical review. *Nanotechnology for Environmental Engineering*, *8*, 377–397. <https://doi.org/10.1007/s41204-022-00276-8>
- Avolio, M., Gavilán, H., Mazario, E., Brero, F., Arosio, P., Lascialfari, A., & Puerto Morales, M. (2019). Elongated magnetic nanoparticles with high-aspect ratio: A nuclear relaxation and specific absorption rate investigation. *Physical Chemistry Chemical Physics: PCCP*, *21*, 18741–18752. <https://doi.org/10.1039/C9CP03441B>
- Beyene, H. D., Werkneh, A. A., Bezabh, H. K., & Ambaye, T. G. (2017). Synthesis paradigm and applications of silver nanoparticles (AgNPs), a review. *Sustainable Materials and Technologies*, *13*, 18–23. <https://doi.org/10.1016/j.susmat.2017.08.001>
- Bhole, R., Gonsalves, D., Murugesan, G., Kumar, M., & Srinivasan, N. N. R. (2023). Superparamagnetic spherical magnetite nanoparticles: Synthesis, characterization and catalytic potential. *Applied Nanoscience*, *13*, 6003–6014. <https://doi.org/10.1007/s13204-022-02532-4>
- Bissessur, R. (2020). *Nanomaterials applications, Polymer Science and Nanotechnology: Fundamentals and Applications*. Elsevier Inc. <https://doi.org/10.1016/B978-0-12-816806-6.00018-2>
- Cartwright, A., Jackson, K., Morgan, C., Anderson, A., & Britt, D. W. (2020). A review of metal and metal-oxide nanoparticle coating technologies to inhibit agglomeration and increase bioactivity for agricultural applications. *Agronomy*, *10*, 1–20. <https://doi.org/10.3390/agronomy10071018>
- Castro-Criado, D., Rivera-Flores, O., Abdullah, J. A. A., Castro-Osorto, E., Alonso-González, M., Ramos-Casco, L., Perez-Puyana, V. M., Sánchez-Barahona, M., Sánchez-Cid, P., Jiménez-Rosado, M., & Romero, A. (2023). Valorization of honduran agro-food waste to produce bioplastics. *Polymers (Basel)*. <https://doi.org/10.3390/polym15122625>
- Cefali, L. C., Cazedey, E. C. L., Souza-Moreira, T. M., Correa, M. A., Salgado, H. R. N., & Isaac, V. L. B. (2015). Antioxidant activity and validation of quantification method for lycopene extracted from tomato. *Journal of AOAC International*, *98*, 1340–1345. <https://doi.org/10.5740/jaoacint.14-151>
- Chandrasekar, N., Mohan Kumar, K. M., Balasubramanian, K. S., Karunamurthy, K., & Varadharajan, R. (2013). Facile synthesis of iron oxide, iron-cobalt and zero valent iron nanoparticles and evaluation of their anti microbial activity, free radicle

- scavenging activity and antioxidant assay. *Digest Journal of Nanomaterials & Biostructures*, 8, 765–775.
- Cruz, R. M., Krauter, V., Agriopoulou, S., Weinrich, R., Herbes, C., Scholten, P. B., Uysal-unalan, I., Sogut, E., Kopacic, S., Lahti, J., Rutkaite, R., & Varzakas, T. (2022). Bioplastics for food packaging: Environmental impact, trends and regulatory aspects. *Foods*, 11, 1–39.
- Fahmy, M. D., Jazayeri, H. E., Razavi, M., Hashemi, M., Omid, M., Farahani, M., Salahinejad, E., Yadegari, A., Pitcher, S., & Tayebi, L. (2016). Biomedical applications of intelligent nanomaterials. *Intelligent Nanomaterials Second Ed*, 13, 199–245. <https://doi.org/10.1002/9781119242628.ch8>
- Fahmy, H. M., Mohamed, F. M., Marzouq, M. H., Mustafa, A. B. E., Alsoudi, A. M., Ali, O. A., Mohamed, M. A., & Mahmoud, F. A. (2018). Review of green methods of iron nanoparticles synthesis and applications. *Bionanoscience*, 8, 491–503. <https://doi.org/10.1007/s12668-018-0516-5>
- Fjellvag, H., Hauback, B. C. B. C., Vogt, T., Stolen, S., & Stølen, S. (2002). Monoclinic nearly stoichiometric wüstite at low temperatures. *American Mineralogist*, 87, 347–349. <https://doi.org/10.2138/am-2002-2-318>
- Fleet, M. E. (1986). The structure of magnetite: Symmetry of cubic spinels. *Journal of Solid State Chemistry*, 62, 75–82.
- Galus, S., Arik Kibar, E. A., Gniewosz, M., & Kraśniewska, K. (2020). Novel materials in the preparation of edible films and coatings—A review. *Coatings*, 10, 674. <https://doi.org/10.3390/coatings10070674>
- Greaves, C. (1983). A powder neutron diffraction investigation of vacancy ordering and covalence in  $\gamma$ -Fe<sub>2</sub>O<sub>3</sub>. *Journal of Solid State Chemistry*, 49, 325–333. [https://doi.org/10.1016/S0022-4596\(83\)80010-3](https://doi.org/10.1016/S0022-4596(83)80010-3)
- Islam, M. R., Kamal, M. M., Kabir, M. R., Hasan, M. M., Haque, A. R., & Hasan, S. M. K. (2023). Phenolic compounds and antioxidants activity of banana peel extracts: Testing and optimization of enzyme-assisted conditions. *Measurement Food*, 10, 100085. <https://doi.org/10.1016/j.meafoo.2023.100085>
- Jamkhande, P. G., Ghule, N. W., Bamer, A. H., & Kalaskar, M. G. (2019). Metal nanoparticles synthesis: An overview on methods of preparation, advantages and disadvantages, and applications. *Journal of Drug Delivery Science and Technology*, 53, 101174. <https://doi.org/10.1016/j.jddst.2019.101174>
- Jeetkar, T. J., Khataokar, S. P., Indurkar, A. R., Pandit, A., & Nimbalkar, M. S. (2022). A review on plant-mediated synthesis of metallic nanoparticles and their applications. *Advances in Natural Sciences: Nanoscience and Nanotechnology*. <https://doi.org/10.1088/2043-6262/ac865d>
- Juby, T. R., Saniya, S., Hariharan, V., & Sreejith, J. (2022). Green synthesis of iron oxide nanoparticles using simarouba glauca leaf extract and application in textile effluent treatment. *International Journal for Research in Applied Science and Engineering Technology*, 10, 3893–3899. <https://doi.org/10.22214/ijraset.2022.43262>
- Jurkow, R., Pokluda, R., Sękara, A., & Kalisz, A. (2020). Impact of foliar application of some metal nanoparticles on antioxidant system in oakleaf lettuce seedlings. *BMC Plant Biology*, 20, 1–12. <https://doi.org/10.1186/s12870-020-02490-5>
- Kanagasubbulakshmi, S., & Kadirvelu, K. (2017). Green synthesis of iron oxide nanoparticles using *Lagenaria siceraria* and evaluation of its antimicrobial activity. *Defence Life Science Journal*, 2, 422. <https://doi.org/10.14429/dlsj.2.12277>
- Kang, Y., Liang, Y., Sun, H., Dan, J., Zhang, Q., Su, Z., Wang, J., & Zhang, W. (2023). Selective enrichment of gram-positive bacteria from apple juice by magnetic Fe<sub>3</sub>O<sub>4</sub> nanoparticles modified with phytic acid. *Food and Bioprocess Technology*, 16, 1280–1291. <https://doi.org/10.1007/s11947-022-02984-0>
- Khoo, H. H., Tan, R. B. H., & Chng, K. W. L. (2010). Environmental impacts of conventional plastic and bio-based carrier bags. *International Journal of Life Cycle Assessment*, 15, 284–293. <https://doi.org/10.1007/s11367-010-0162-9>
- Kibria, M. G., Masuk, N. I., Safayet, R., Nguyen, H. Q., & Mourshed, M. (2023). Plastic waste: Challenges and opportunities to mitigate pollution and effective management. *International Journal of Environmental Research*. Springer International Publishing. <https://doi.org/10.1007/s41742-023-00507-z>
- Koller, M., Hesse, P., Kutschera, C., Bona, R., Nascimento, J., Ortega, S., Agnelli, J. A., & Braunnegg, G. (2009). Sustainable embedding of the bioplastic poly-(3-hydroxybutyrate) into the sugarcane industry: principles of a future-oriented technology in Brazil. *Polymers - opportunities and risks II* (pp. 81–96). Berlin, Heidelberg: Springer. [https://doi.org/10.1007/698\\_2009\\_11](https://doi.org/10.1007/698_2009_11)
- Konwar, A., Kalita, S., Kotoky, J., Chowdhury, D., Kloster, G. A., Mosiewicki, M. A., Marcovich, N. E., Susilowati, E., Maryani Ashadi, M., Rhim, J. W., Hong, S. I., Park, H. M., Ng, P. K. W., Bertuzzi, M. A., Castro Vidaurre, E. F., Armada, M., Gottifredi, J. C., Vimala, K., Mohan, Y. M., ... Heredia-Guerrero, J. A. (2020). Water vapor permeability of edible starch based films. *Nanomaterials*, 14, 5761–5773. <https://doi.org/10.3390/POLYM12040942>
- Manzo, M., Ahmed, H., & Nasrazadani, S. (2020). Study on emission spectral lines of hematite and magnetite for purity's differentiation. *Aip Advances*. <https://doi.org/10.1063/1.5143413>
- Modi, A. A., Shahid, R., Saeed, M. U., & Younas, T. (2018). Hemp is the future of plastics. *E3S Web of Conferences*, 51, 03002. <https://doi.org/10.1051/e3sconf/20185103002>
- Mohammed, H. A., Eddine, L. S., Souhaila, M., Hasan, G. G., Kir, I., & Abdullah, J. A. A. (2023). Green synthesis of SnO<sub>2</sub> nanoparticles from laurus nobilis L. extract for enhanced gelatin-based films and CEF@SnO<sub>2</sub> for efficient antibacterial activity. *Food And Bioprocess Technology*. <https://doi.org/10.1007/s11947-023-03209-8>
- Momotaz, F., Sarkar, A., Hasan, N., & Chowdhury, H. K. (2022). Development of biodegradable plastics from potato starch with enhanced physico-mechanical properties comparative to the regular plastic. In: *Breaking boundaries*. Iowa State University Digital Press. <https://doi.org/10.31274/itaa.13732>
- Nalbandian, L., Patrikiadou, E., Zaspalis, V., Patrikidou, A., Hatzidaki, E., & Papatreou, N. (2015). Magnetic nanoparticles in medical diagnostic applications: Synthesis, characterization and proteins conjugation. *Current Nanoscience*, 12, 455–468. <https://doi.org/10.2174/1573413712666151210230002>
- Nandiyanto, A. B. D., Oktiani, R., & Ragadhita, R. (2019). How to read and interpret FTIR spectroscopy of organic material. *Indonesian Journal Science and Technology*, 4, 97. <https://doi.org/10.17509/ijost.v4i1.15806>
- Onen Cinar, S., Chong, Z. K., Kucuker, M. A., Wiczorek, N., Cengiz, U., & Kuchta, K. (2020). Bioplastic production from microalgae: A review. *International Journal of Environmental Research and Public Health*, 17, 3842. <https://doi.org/10.3390/ijerph17113842>
- Pardo, L., Arias, J., & Molleda, P. (2022). Preparation of synthesized silver nanoparticles from extract of rosemary leaves (*rosmarinus officinalis* L.) and its used as a preservative. *Granja*, 35, 45–58. <https://doi.org/10.17163/lgr.n35.2022.04>
- Park, B., Kim, B. H., & Yu, T. (2018). Synthesis of spherical and cubic magnetic iron oxide nanocrystals at low temperature in air. *Journal of Colloid and Interface Science*, 518, 27–33. <https://doi.org/10.1016/j.jcis.2018.02.026>
- Patni, N., Yadava, P., Agarwal, A., & Maroo, V. (2014). An overview on the role of wheat gluten as a viable substitute for biodegradable plastics. *Reviews in Chemical Engineering*, 30, 421–430. <https://doi.org/10.1515/revce-2013-0039>
- Patra, J. K., & Baek, K. H. (2017). Green biosynthesis of magnetic iron oxide (Fe<sub>3</sub>O<sub>4</sub>) nanoparticles using the aqueous extracts of food processing wastes under photo-catalyzed condition and investigation of their antimicrobial and antioxidant activity. *Journal*

- of *Photochemistry and Photobiology B Biology*, 173, 291–300. <https://doi.org/10.1016/j.jphotobiol.2017.05.045>
- Phothisarattana, D., Wongphan, P., Promhuad, K., Promsorn, J., & Harnkarnsujarit, N. (2021). Biodegradable poly(butylene adipate-co-terephthalate) and thermoplastic starch-blended TiO<sub>2</sub> nanocomposite blown films as functional active packaging of fresh fruit. *Polymers (Basel)*, 13, 4192. <https://doi.org/10.3390/polym13234192>.
- Rahman, M. M., Dey, A., Yodo, N., Lee, C. W., & Grewell, D. (2023). Soybean by-products bioplastic (polylactic acid)-based plant containers: Sustainable development and performance study. *Sustainability*, 15, 5373. <https://doi.org/10.3390/su15065373>.
- Rajakumar, G., Thiruvengadam, M., Mydhili, G., Gomathi, T., & Chung, I. M. (2018). Green approach for synthesis of zinc oxide nanoparticles from *Andrographis paniculata* leaf extract and evaluation of their antioxidant, anti-diabetic, and anti-inflammatory activities. *Bioprocess and Biosystems Engineering*, 41, 21–30. <https://doi.org/10.1007/s00449-017-1840-9>.
- Rajeswari, V. D., Khalifa, A. S., Elfasakhany, A., Badruddin, I. A., Kamangar, S., & Brindhadevi, K. (2021). Green and ecofriendly synthesis of cobalt oxide nanoparticles using phoenix dactylifera L: antimicrobial and photocatalytic activity. *Applied Nanoscience*. <https://doi.org/10.1007/s13204-021-02038-5>
- Ramananda, H. S. M., Senthil, B. P., Kumar, N. M., & Selvaraj, R. (2023). Structural characterization of cuboidal  $\alpha$ -Fe<sub>2</sub>O<sub>3</sub> nanoparticles synthesized by a facile approach. *Applied Nanoscience*, 13, 5605–5613. <https://doi.org/10.1007/s13204-023-02780-y>
- Rana, A., Yadav, K., & Jagadevan, S. (2020). A comprehensive review on green synthesis of nature-inspired metal nanoparticles: Mechanism, application and toxicity. *Journal of Cleaner Production*, 272, 122880. <https://doi.org/10.1016/j.jclepro.2020.122880>.
- Salgado, P., Márquez, K., Rubilar, O., Contreras, D., & Vidal, G. (2019). The effect of phenolic compounds on the green synthesis of iron nanoparticles (Fe<sub>x</sub>O<sub>y</sub>-NPs) with photocatalytic activity. *Appl Nanosci*, 9, 371–385. <https://doi.org/10.1007/s13204-018-0931-5>.
- Santoyo Salazar, J., Perez, L., De Abril, O., Truong Phuoc, L., Ihiawakrim, D., Vazquez, M., Greneche, J. M. M., Begin-Colin, S., & Pourroy, G. (2011). Magnetic iron oxide nanoparticles in 10–40 nm range: Composition in terms of magnetite/maghemite ratio and effect on the magnetic properties. *Chemistry of Materials*, 23, 1379–1386. <https://doi.org/10.1021/cm103188a>.
- Sharmiladevi, S., Ramesh, N., & Ramesh, S. (2019). Production of bio degradable bags using cassava starch. *International Research Journal of Multidisciplinary Technovation*. <https://doi.org/10.34256/irjmtcon80>
- Simol, H., Sultana, R., Mollah, M. Y. A., & Miran, M. (2020). Synthesis of Fe<sub>3</sub>O<sub>4</sub> and Fe<sub>2</sub>O<sub>3</sub> nanoparticles using hybrid electrochemical-thermal method. *Bangladesh Journal of Scientific and Industrial Research*, 55, 221–228. <https://doi.org/10.3329/bjsir.v55i3.49396>
- Tadic, M., Trpkov, D., Kopanja, L., Vojnovic, S., & Panjan, M. (2019). Hydrothermal synthesis of hematite ( $\alpha$ -Fe<sub>2</sub>O<sub>3</sub>) nanoparticle forms: Synthesis conditions, structure, particle shape analysis, cytotoxicity and magnetic properties. *Journal of Alloys and Compounds*, 792, 599–609. <https://doi.org/10.1016/j.jallcom.2019.03.414>.
- Tuoriniemi, J., Johnsson, A. C. J. H., Holmberg, J. P., Gustafsson, S., Gallego-Urrea, J. A., Olsson, E., Pettersson, J. B. C., & Hassellöv, M. (2014). Intermethod comparison of the particle size distributions of colloidal silica nanoparticles. *Science and Technology of Advanced Materials*. <https://doi.org/10.1088/1468-6996/15/3/035009>.
- Üstün, E. (2021). Green synthesis of iron oxide nanoparticles by using ficus carica leaf extract and its antioxidant activity. *Biointerface Research in Applied Chemistry*, 12, 2108–2116. <https://doi.org/10.33263/BRIAC122.21082116>
- Venkateswarlu, S., Natesh Kumar, B., Prasad, C. H., Venkateswarlu, P., & Jyothi, N. V. V. (2014). Bio-inspired green synthesis of Fe<sub>3</sub>O<sub>4</sub> spherical magnetic nanoparticles using syzygium cumini seed extract. *Physica B Condensed Matter*, 449, 67–71. <https://doi.org/10.1016/j.physb.2014.04.031>
- Vinayagam, R., Nagendran, V., & Concepta, L. (2024). Structural characterization of marine macroalgae derived silver nanoparticles and their colorimetric sensing of hydrogen peroxide. *Materials Chemistry and Physics*, 313, 128787. <https://doi.org/10.1016/j.matchemphys.2023.128787>.
- Wang, T., Jin, X., Chen, Z., Megharaj, M., & Naidu, R. (2014a). Science of the total Environment Green synthesis of Fe nanoparticles using eucalyptus leaf extracts for treatment of eutrophic wastewater. *Science of the Total Environment*. <https://doi.org/10.1016/j.scitotenv.2013.07.022>.
- Wang, Z., Fang, C., & Megharaj, M. (2014b). Characterization of iron-polyphenol nanoparticles synthesized by three plant extracts and their fenton oxidation of azo dye. *Acs Sustainable Chemistry & Engineering*, 2, 1022–1025. <https://doi.org/10.1021/sc500021n>.
- Wright, J. P., Attfield, J. P., & Radaelli, P. G. (2002). Charge ordered structure of magnetite. *Physical Review B, Condensed Matter*, 66, 214422. <https://doi.org/10.1103/PhysRevB.66.214422>.
- Zhang, S., Wu, W., Xiao, X., Zhou, J., Ren, F., & Jiang, C. (2011). Preparation and characterization of spindle-like Fe<sub>3</sub>O<sub>4</sub> mesoporous nanoparticles. *Nanoscale Research Letters*, 6, 89. <https://doi.org/10.1186/1556-276X-6-89>.
- Zounggran, Y., Lynda, E., Dobi-Brice, K. K., Tchirioua, E., Bakary, C., & Yannick, D. D. (2020). Influence of natural factors on the biodegradation of simple and composite bioplastics based on cassava starch and corn starch. *Journal of Environmental Chemical Engineering*, 8, 104396. <https://doi.org/10.1016/j.jece.2020.104396>

**Publisher's Note** Springer Nature remains neutral with regard to jurisdictional claims in published maps and institutional affiliations.